Review Article

Guojun Jiang, Lee Johnson, and Sheng Xie*

Investigations into the mechanisms of electrohydrodynamic instability in free surface electrospinning

https://doi.org/10.1515/phys-2019-0033
Received Apr 10, 2019; accepted Apr 30, 2019

Abstract: Free surface electrospinning is a continuous electrospinning method for low-cost, massive production of nanofibers. The interjet distance λ is a critical parameter in free surface electrospinning, which directly determines the nanofiber production efficiency. In this investigation, we studied the interjet distance during free surface electrospinning based on electrohydrodynamic instability theoretically and experimentally, with special interest focused on the effect of surface tension and electric field intensity on the interjet distance. The experimental results indicated that the critical parameters affecting the interjet distance were the surface tension and applied voltage, which was in good compliance with the theoretical prediction. The relationship between interjet distance λ and surface tension followed an allometric law with positive exponential function, and the relationship between interjet distance λ and applied voltage followed an allometric law with negative exponential function. The present results can be used to understand the basic parameters which determine the interjet distance in free surface electrospinning.

Keywords: electrospinning; free surface; multiple jets; mechanism

PACS: 47.65.-d, 68.35.Ja, 81.20.-n, 81.70.-q

1 Introduction

Electrospinning technique is a simple and versatile technique to produce continuous nanofibers with many outstanding characteristics, such as high porosity, high ratio of surface area to mass and small pore size etc. [1]. Owing to these useful properties, electrospun nanofibers have various applications in various fields, such as filtration, tissue engineering scaffolds, drug delivery devices, protective clothing, sensors, and energy storage [2]. However, the typical low productivity of traditional single needle electrospinning inhibits the industrial development and commercial applications of electrospun nanofibers.

Over the last decade, free surface electrospinning has gained great interest in academic research and attracted more and more commercial attention as it is an effective and promising approach to massive production of nanofibers. Free surface electrospinning is a novel electrospinning technique for massive production of nanofibers, which is based on electrohydrodynamic jetting from the free surface of a polymeric solution or melt. Jirsak *et al.* described a free surface electrospinning setup using a rotating cylinder as the nanofiber generator, which has been commercialized by Elmarco Inc. under the brand name Nanospider [3]. Liu *et al.* employed a gas pump to generate bubbles on a liquid surface to initiate the electrospinning process [4]. Wang *et al.* used multiple ring as spinneret to produce nanofiber with super-high throughput [5]. Thoppey *et al.* reported a simple geometry for high throughput electrospinning from a bowl edge that utilized a vessel filled with a polymer solution [6]. Jiang *et al.* demonstrated a simple and efficient free surface electrospinning setup used to issue multiple jets [7]. Rutledge *et al.* reported the formation of multiple jets from a rotating wire electrode spindle [8]. Higham *et al.* presented a novel technique of free surface electrospinning utlitizing foams [9]. Holopainen *et al.* developed a twisted metal wire as the spinneret to improve the production rate [10]. Liu *et al.* presented a new approach using needle-disk as spinneret to enhance nanofiber throughput and maintain

***Corresponding Author: Sheng Xie:** College of Material and Textile Engineering, Jiaxing University, No.118 Jiahang Road. Jiaxing, 314000, China; Email: shengxie16@163.com
Guojun Jiang: Zhijiang College, Zhejiang University of Technology, No.958 Yuezhou Road, Keqiao, Shaoxing, 312000, China
Lee Johnson: Department of Physics, North Carolina State University, North Carolina 27695, Raleigh, United States of America

high quality nanofiber [11]. Ali *et al.* reported a sprocket wheel disk and a popular mace-shaped spinneret for large-scale production of nanofibers [12, 13]. Yan *et al.* curved slot demonstrated a novel slot electrospinning with curved slot and investigated the effects of slot line shape on electrospinning process [14]. Zheng *et al.* used a threaded rod electrode as the needleless spinneret to achieve high-efficiency production of nanofibers [15].

In the free surface electrospinning process, the interjet distance λ determined the distance between neighbouring jets emitted from the free liquid surface, which directly decides the productivity per unit spinning area. Therefore, the interjet distance λ is a critical parameter of production effectiveness of electrospinning technology from free liquid surfaces. It is noteworthy that the study of the interjet distance λ would provide insight into the mechanisms of electrohydrodynamic instability in free surface electrospinning.

Numerous theoretical models have been reported in the literature regarding the three stages of needle electrospinning process: jet initiation, stretching, and whipping stability. In contrast, only a few theoretical works have been made in the literature regarding the free surface electrospinning. Lukas *et al.* firstly explained self-organization of jets on one-dimensional free liquid surfaces in terms of electrohydrodynamic instability of surface waves [16]. Thoppey *et al.* utilized a simple model to explain the basic parameters which determine the maximum jet number in unconfined electrospinning [17]. Roman *et al.* investigated the role of interjet interactions on maximizing spontaneous jet density in unconfined electrospinning [18]. Jirsak *et al.* used Monte Carlo and molecular dynamics simulations to model the electrospinning process from the free liquid surface [19]. Kula *et al.* designed a unique computer vision system and digital image processing to track position of every polymer jet from free liquid surface electrospinning [20]. Li *et al.* presented a detailed theoretical analysis of interjet distance in needleless melt differential electrospinning [21].

In our free surface electrospinning process, multiple jets can be formed simultaneously from the free surface when the electric force overcame the surface tension. In the initial stage, small perturbation on the liquid free surface causes the polymer solution to form into many cone like spikes, which closely resembles the electrohydrodynamic instabilities to thin polymer films. From the physical point of view, the free surface electrospinning process represents the problem of the behaviour of air liquid interface exposed to external electric fields. To date, numerous theoretical studies have been performed to investigate the electrohydrodynamic destabilization of the thin polymer films. Such theoretical studies on electrohydrodynamic instabilities might provide great insight into understanding the mechanisms of free surface electrospinning.

In this work, we aim to extend the application of electrohydrodynamics for analyzing the evolution of instabilities from a polymer solution in free surface electrospinning process. A simple model was formulated based on electrohydrodynamic theory to investigate the behaviour of multiple Taylor cones in free surface electrospinning. Furthermore, the effect of surface tension and electric field intensity on the interjet distance λ were discussed. The model is validated by extensively comparing the numerical simulations with experimental data. Therefore, the simple model is helpful in understanding the mechanisms of free surface electrospinning.

2 Experimental details

2.1 Materials

Polyvinyl alcohol (PVA) with an average molecular weight of 95,000 g/mol (Acros), a nonionic surfactant Triton X-100 (Sigma-Aldrich), and a dye molecule Rhodamine B (RhB) (Sinopharm Chemical Reagent) were purchased. RhB was used to tint the polymer fluid for better image contrast. Homogeneous 8 wt% PVA solution at various concentrations of Triton X-100 were prepared by dissolving PVA powder in deionized water under the aid of mechanical stirring for 8 h at 80°C in order to obtain a wide range of solution surface tensions.

2.2 Characterization

The solution surface tension was evaluated using the Wilhelmy-plate method by a surface tension meter (Shanghai Fangrui Instrument Corp, QBZY-2). The motion of multiple jets during the free electrospinning process were captured by a digital camera (Cannon, 650D). In order to correctly calculate the jets number, we only electrospun from the semi-circumference of the stepped pyramid spinneret and visualized the jet formation process from a side view perspective.

The electric field distribution around the spinneret surface was calculated by the commercially available software (Maxwell 3D, ANSOFT Corp.). The actual model of the free surface electrospinning setups was established based on the physical size of apparatus.

2.3 Free surface electrospinning

The experiments were carried out on a free surface electrospinning setup. The schematic of the free surface electrospinning system is shown in Figure 1, which contained five major components: a high-voltage direct-current power supply, a stepped pyramid stage, a Teflon solution reservoir, a pump, and a grounded collector. 'A' was utilized as the electrospinning generator.

During the free surface electrospinning, the solution was continuously pumped into the stepped pyramid stage so that every edge of the stepped pyramid stage was covered with the polymer solution; meanwhile, the excessive solution was made to flow slowly to the reservoir. The applied voltage was increased until a number of jets were observed simultaneously from every edge. The PVA solutions were electrospun at different applied voltages, and the working distance (the distance between the top lip of the stepped pyramid stage and the grounded collector), was set as 15 cm, respectively. The experiments were carried out at room temperature in the air.

3 Results and discussion

3.1 Electric field modeling

The electric field distribution profile of the spinneret directly affects the free surface electrospinning performance. As shown in Figure 2, the electric field intensity profile simulation results indicated that the electric field evenly distributed on every edge of the stepped pyramid stage, from the uppermost edge to the bottommost edge. The maximum electric field strength was formed on the curving part of the free surface, suggesting that those sites are more efficient to self-generate jets.

3.2 A simple model for free surface electrospinning

Based on the above electric field analysis, we only consider a single half-periodic stage of the stepped pyramid stage in this work to simplify our problem. The three-dimensional electrohydrodynamic phenomenon of the free surface electrospinning with stepped pyramid stage can be simplified to one-dimensional model as shown in Figure 3.

According to the Navier–Stokes equation, the motion of the fluid can be described as the following equation:

$$\rho\frac{\partial v}{\partial t}+\rho(v\cdot\nabla)v=-\nabla p+\eta\Delta v+(\eta+\frac{1}{3}\lambda)\nabla(\nabla\cdot v)+f \quad (1)$$

Because the polymer fluid viscosities are high and the velocity gradients are very small, the convective term can be neglected. Moreover, the dynamics of the polymer fluid is very slow and the velocity profile can be always considered in quasi–steady–state. Then the Navier–Stokes equation can be simplified as

$$0=-\nabla P+\eta\nabla^2 v \quad (2)$$

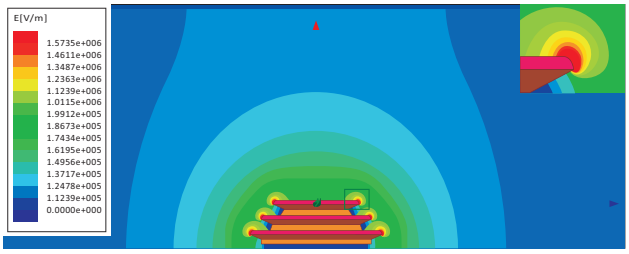

Figure 1: Scheme of the electrospinning apparatus using a stepped pyramid stage

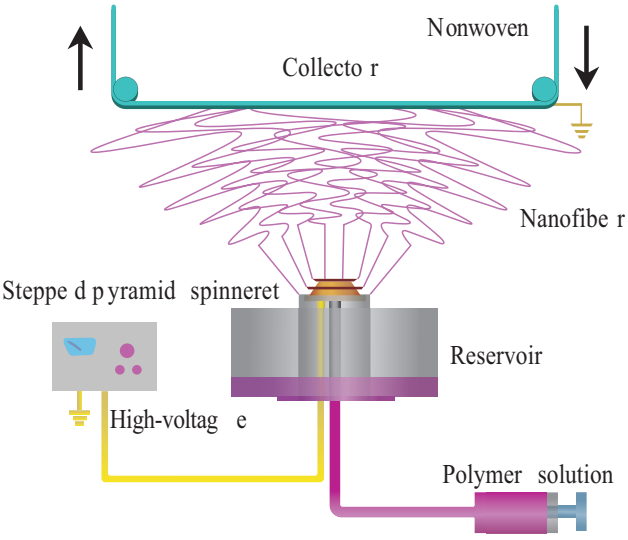

Figure 2: Simulation of electric field distribution

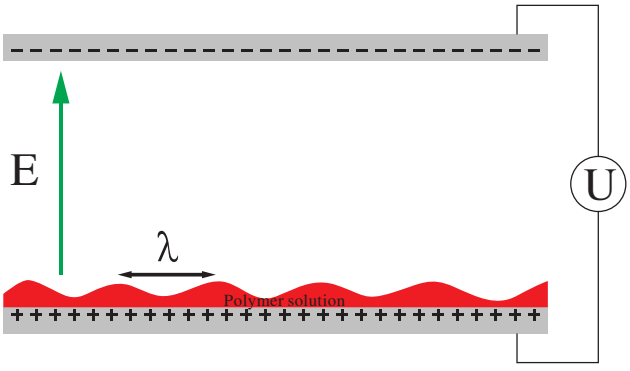

Figure 3: Schematic representation of electrohydrodynamic instability

At the free interface, the internal stresses within the liquid must be counterbalanced by external stresses due to surface forces. Then the condition can be represented as

$$\eta_{liquid} \cdot \partial_z v_{liquid}(z) = \eta_{air} \cdot \partial_z v_{air}(z) \tag{3}$$

Because no stresses can exist at the free interface, the stress at the interface is equal to zero. Eq. (3) becomes

$$\sigma_{xz} = \eta \partial_z v_{liquid}(z) = 0 \tag{4}$$

Considering only the velocity vector in the x–direction is non–zero, the Eq. (4) as a function of the z–coordinate can be expressed as

$$\partial_{zz} v(z) = \frac{1}{\eta}(\partial_x P) \tag{5}$$

Then integral can be obtained as

$$v(z) = \frac{1}{2\eta}(\partial_x P) \cdot z^2 + c_1 \cdot z + c_2 \tag{6}$$

The constants c_1 and c_2 can be obtained by the boundary conditions.

In our model, there is no liquid motion relative to the stepped pyramid stage, and the free interface is a free pressure liquid surface. The boundary conditions can be described as

$$z = \begin{cases} 0 : v = 0 \\ h : \sigma = \eta v_z = 0 \end{cases} \tag{7}$$

Using these initial conditions, the constants c_1 and c_2 in Eq. (6) are easily computed. Then the velocity distribution becomes

$$v(z) = \frac{1}{2\eta}(\partial_x P)(z - 2h)z \tag{8}$$

and the average velocity of solution is calculated as

$$\overline{v} = \frac{1}{h}\int_0^h v(z)dz = \frac{h^2}{3\eta}(-\partial_x P) \tag{9}$$

In our one-dimensional model, the flux j on the surface of A=h can be calculated as

$$j = \frac{h^3}{3\eta}(-\frac{\partial p}{\partial x}) \tag{10}$$

In terms of the mass–conservation law, the incompressible fluid is given by the following equation:

$$(h \cdot \overline{v})_{x+dx} - (h \cdot \overline{v})_x = \partial_x (h \cdot \overline{v}) dx \tag{11}$$

with $h \cdot \overline{v} = j$

$$\frac{\partial j}{\partial x} + \frac{\partial h}{\partial t} = 0 \tag{12}$$

Combined with Eq. (10) and Eq. (12), the equation of motion for the free surface can be described as

$$\partial_t h = \partial_x \left[\frac{h^3}{3\eta}(\partial_x P)\right] \tag{13}$$

On the basis of electrohydrodynamics, a general discussion of free surface instability due to an external electric force has been previously investigated [22]. The overall pressure P on the free surface is given by the sum of two main contributions: the surface tension and the electric force. In this case, the external electric field serves as the driving force to create fluid perturbations, and the surface tension resists deformation of the fluid. The overall pressure distribution at the free surface can be expressed as

$$P(h) = P_L(h) + P_{el}(h) \tag{14}$$

where the Laplace pressure due to the surface tension can be calculated as $P_L(h) = -\partial_{xx} h$; the second term is the electrostatic pressure which is produced by high voltage electric field, and can be calculated as$p_{el} = \frac{1}{2}\varepsilon E^2$.

Numerous theoretical studies have been reported that linear stability analysis of surface instability can be used to predict the wavelength λ on the polymer-air interface [22]. In this work, we model the wavelike perturbation of the polymer-air interface as

$$h(x,t) = h_0 + \zeta e^{iqx + \frac{t}{\tau}} \tag{15}$$

where h_0 is the initial thickness, ζ is the perturbation amplitude, q is the wave vector, τ is the time constant, t is the time, and x is the lateral coordinate parallel to the surface.

After derivation, the Eq. (15) results in

$$\begin{aligned} \partial_t h &= \frac{h^2}{\eta}(\partial_x h)[\partial_x P] + \frac{h^3}{3\eta}[\partial_{xx} P] \\ &= \frac{h^2}{\eta}(\partial_x h)[-\gamma(\partial_{xxx} h) + (\partial_h P_{el})(\partial_x h)] \\ &+ \frac{h^3}{3\eta}\left[-\gamma(\partial_{xxxx} h) + (\partial_{hh} P_{el})(\partial_x h)^2 + (\partial_h P_{el})(\partial_{xx} h)\right] \end{aligned} \tag{16}$$

simplifies to

$$\partial_t h = \frac{h^3}{3\eta}\left[-\gamma(\partial_{xxxx} h) + (\partial_h p_{el})(\partial_{xx} h)\right] + O(\zeta^2) \tag{17}$$

After calculating the partial derivatives in Eq. (17) and dividing by$\zeta \exp(iqx + t/\tau)$, we can get:

$$\frac{1}{\tau} = -\frac{h^3}{3\eta}\left[\gamma q^4 + q^2 \partial_h p_{el}\right] \tag{18}$$

When $q_{\max} = \sqrt{-\frac{\partial_h p_{el}}{2\gamma}}$, the characteristic wavelength is

$$\lambda_{\max} = 2\pi\sqrt{\frac{-2\gamma}{\partial_h p_{el}}} \tag{19}$$

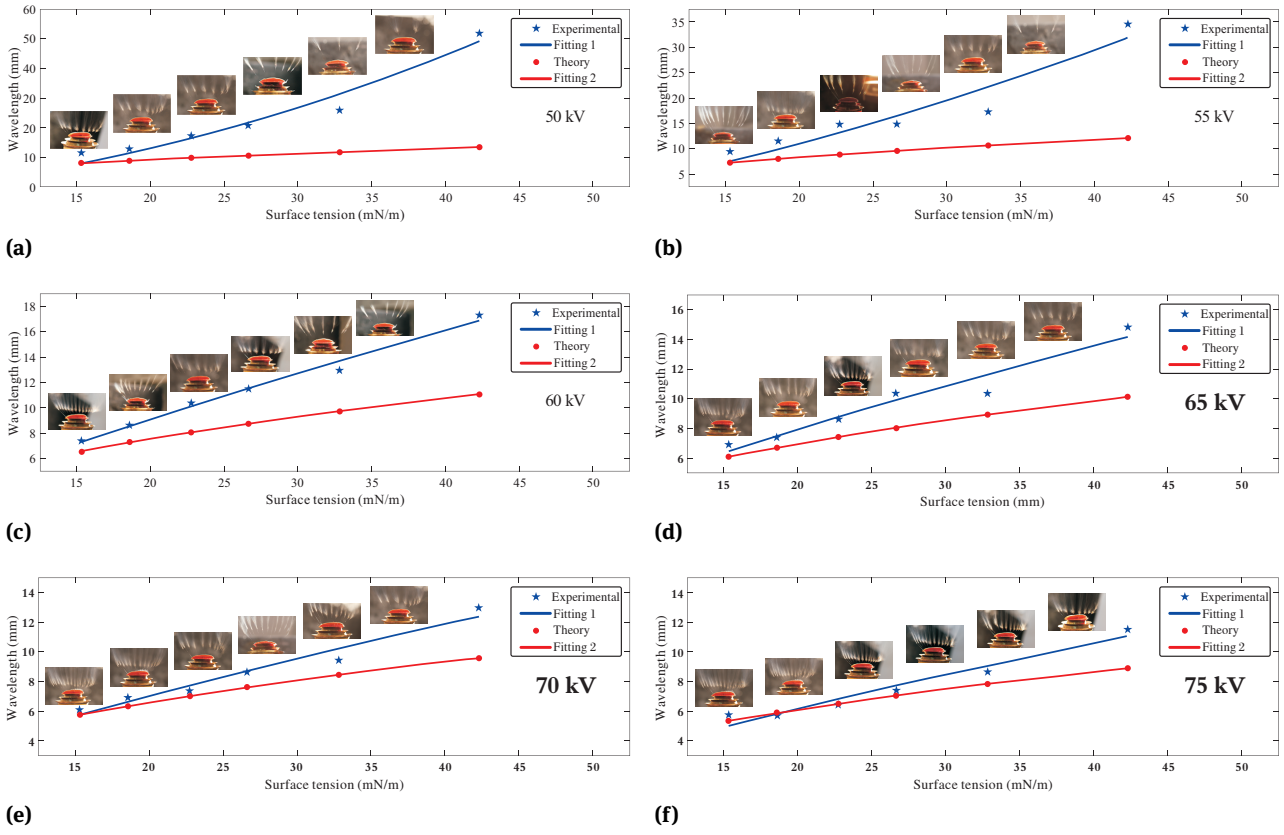

Figure 4: Experimentally and theoretically interjet distance as a function of the surface tension at different applied voltage: (a) 50 kV; (b) 55 kV; (c) 60 kV; (d) 65 kV; (e) 70 kV; (f) 75 kV

Then the form of an allometric relation between wavelength λ and surface tension γ, wavelength λ and applied voltage can be expressed as

$$\lambda \propto \gamma^{\frac{1}{2}} \tag{20}$$

$$\lambda \propto U^{-1} \tag{21}$$

3.3 Effect of surface tension on interjet distance in ferr surface electrospinning

In free surface electrospinning, the evolution of the air-polymer interface is driven by the competition between the electrostatic pressure and the Laplace pressure. The surface tension of the polymer will try to stabilize the free surface, which resists deformation of the polymer.

In this study, the effect of surface tension on interjet distance λ in free surface electrospinning was investigated by adding different amounts of Triton X-100 with other parameters kept the same. Figure 4 shows experimental and theoretical wavelength as a function of the surface tension at different applied voltages. Comparing the morphologies in Figure 4 clearly shows that changing the surface tension has a noticeable effect on interjet distance λ in free surface electrospinning. As the surface tension increases, longer interjet distances are obtained from both the experimental results and theoretical models, resulting in less jets generated in free surface electrospinning process. In contrast, a lower surface tension will decrease the interjet distance λ. It could be explained that increasing the surface tension will generates a larger Laplace pressure along the air-polymer interface and needs a larger electrostatic pressure to overcome it, thus resulting in less deformation of the solution surface. Figure 4 also shows that the increment of the applied voltage is observed to decrease the scaling exponent, which gradually approach to agree well with the theoretical model.

3.4 Effect of applied voltage on interjet distance in ferr surface electrospinning

In free surface electrospinning, the polymer solution is electrically charged, and the electrostatic force will polar-

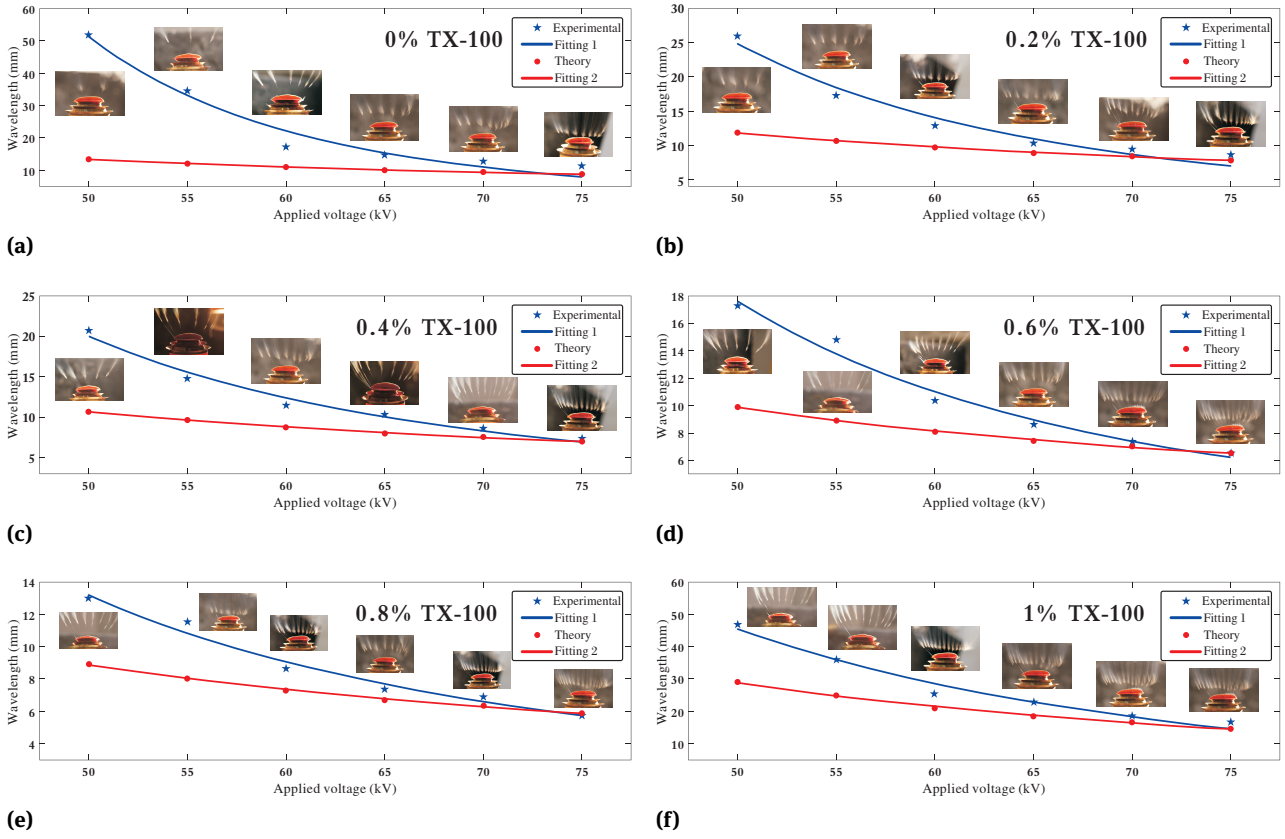

Figure 5: Experimentally and theoretically interjet distance as a function of the applied voltage at different surface tension: (a) 0% TX-100; (b) 0.2% TX-100; (c) 0.4% TX-100; (d) 0.6% TX-100; (e) 0.8% TX-100; (f) 1% TX-100

ize the polymer, thus the electric field serves as the outwardly driving force to create the deformation of the polymer solution.

In this study, the effect of applied voltage on interjet distance λ in free surface electrospinning, was investigated. Figure 5 shows experimental and theoretical interjet distance as a function of the applied voltage with different surface tensions. As can be seen, long interjet distance are obtained from both the experimental results and theoretical models under a low applied voltage. As the applied voltage increases, the deformation of the free surface gets significant, consequently, resulting in more jets generated in free surface electrospinning process. Referring to Figure 5, the deformation gets pronounced when the applied voltage is 60 kV or above. It can be explained that a higher applied voltage generates a larger electrostatic pressure along the air-polymer interface and needs a larger Laplace pressure to balance it, thus resulting in a more severe deformation in free surface electrospinning process. Another phenomenon observed is that the coincidence between experimental results and theoretically prediction is sensitive to surface tension. Specifically, a small increase of intensity causes a large rise of interface deformation.

4 Conclusions

In this work, a simple one-dimensional model was formulated based on electrohydrodynamic theory to investigate the evolution of instabilities from a polymer solution in free surface electrospinning process. The relationship between interjet distance λ and surface tension followed an allometric law in the form of $\lambda \propto \gamma^{\frac{1}{2}}$, and the relationship between interjet distance λ and applied voltage followed an allometric law in the form of $\lambda \propto U^{-1}$. Experimental research demonstrated that the surface tension of the polymer and applied voltage both have a significant influence on interjet distance λ in free surface electrospinning. It was found that the theoretically calculated results were close to experimental results, especially with low surface tension and high applied voltage providing the highest throughput. The experimental interjet distance was a

little larger than theoretically calculated value. There are some possible reasons for the discrepancy between experimental results and our theoretical prediction, such as the ignorance of solution viscosity in our simple model and the electric field intensity profile from electric field simulations. Therefore, further research should be done to study the mechanism of this free surface electrospinning system.

Acknowledgement: This work was supported by the National Natural Science Foundation of China (Grant: 11702113), Zhejiang Provincial Natural Science Foundation (Grant: LQ18E030013 and LQ18E030014), Scientific Research Project of Zhejiang Provincial Education Department (Grant: Y201636479).

References

[1] Xue J.J., Xie J.W., Liu W.Y. and Xia Y.N., Electrospun Nanofibers: New Concepts, Materials, and Applications, Accounts Chem Res., 2017, 50, 1976–1987.

[2] Ahmed F.E., Lalia B.S. and Hashaike R., A review on electrospinning for membrane fabrication: Challenges and applications, Desalination., 356 2015, 356, 15–30.

[3] Yalcinkaya F., Yalcinkaya B. and Jirsak O., Analysis of the effects of rotating roller speed on a roller electrospinning system, Text Res J., 2017, 87, 913–928.

[4] Liu F.J., He J.H., Chen R.X., Xu L. and Wang P., Fabrication of nanoporous fibers via bubble electrospinning, Therm Sci., 2014, 18, 1455–1458.

[5] Wang X., Lin T. and Wang X.G., Scaling up the production rate of nanofibers by needleless electrospinning from multiple ring, Fiber Polym., 2014, 15, 961–965.

[6] Thoppey N.M., Bochinski J.R., Clarke L.I., and Gorga R.E., Edge electrospinning for high throughput production of quality nanofibers, Nanotechnology., 2011, 22, 1–11.

[7] Jiang G.J., Zhang S., Wang Y.T. and Qin X.H., An improved free surface electrospinning with micro-bubble solution system for massive production of nanofibers, Mater Lett., 2015, 144, 22–25.

[8] Bhattacharyya I., Molaro M.C., Braatz R.D. and Rutledge G.C., Free surface electrospinning of aqueous polymer solutions from a wire electrode, Chem Eng J., 2015, 289, 203–211.

[9] Higham A.K., Tang C., Landry A.M., Pridgeon M.C., Lee E.M., Andrady A.L. and Khan S.A., Foam electrospinning: A multiple jet, needleless process for nanofiber production, Aiche J., 2014, 60, 1355–1364.

[10] Holopainen J., Penttinen T., Santala E. and Ritala M., Needleless electrospinning with twisted wire spinneret, Nanotechnology., 2015, 26, 1–8.

[11] Liu Z., Chen R.X. and He J.H., Active generation of multiple jets for producing nanofibres with high quality and high throughput, Mater Design., 2016, 94, 496–501.

[12] Ali U., Niu H.T., Aslam S., Jabbar A., Rajput A.W. and Lin T., Needleless electrospinning using sprocket wheel disk spinneret, J Mater Sci., 2017, 52, 7567–7577.

[13] Ali U., Niu H.T., Khurshid M.H., Abbas A. and Lin T., Electrospinning behavior of needleless spinneret with a popular mace shape, J Tex I., 2018,1–9.

[14] Yan G.L., Niu H.T., Shao H., Zhao X.T., Zhou H. and Lin T., Curved convex slot: an effective needleless electrospinning spinneret. J Mater Sci., 2017, 52, 11749–11758.

[15] Zheng G.F., Jiang J.X., Wang X., Li W.W., Zhong W.Z. and Guo S.M., Self-cleaning threaded rod spinneret for highefficiency needleless electrospinning. Appl Phys A-Mater., 2018, 124, 473–480.

[16] Lukas D., Sarkar A. and Pokorny P., Self-organization of jets in electrospinning from free liquid surface: A generalized approach, J Appl Phys., 2008, 103, 1–7.

[17] Thoppey N.M., Gorga R.E., Bochinski J.R. and Clarke L.I., Effect of Solution Parameters on Spontaneous Jet Formation and Throughput in Edge Electrospinning from a FluidFilled Bowl, Macromolecules., 2012, 45, 6527–6537.

[18] Roman M.P., Thoppey N.M., Gorga R.E., Bochinski J.R. and Clarke L.I., Maximizing Spontaneous Jet Density and Nanofiber Quality in Unconfined Electrospinning: The Role of Interjet Interactions. Macromolecules., 2013, 46, 7352–7362.

[19] Jirsak J., Moucka F. and Nezbeda I., Insight into Electrospinning via Molecular Simulations, Ind Eng Chem Res., 2014, 53, 8257–8264.

[20] Kula J., Linka A., Tunak M. and Lucas D., Image analysis of jet structure on electrospinning from free liquid surface, Appl. Phys. Lett., 2014, 104, 1–4.

[21] Li H.Y., Chen H.B., Zhong X.F., Wu W.F., Wu Y.M. and Yang W.M., Interjet distance in needleless melt differential electrospinning with umbellate nozzles, J App Polym Sci., 2014, 131, 1–8.

[22] Holgate J.T., Coppins M. and Allen J.E., Electrohydrodynamic stability of a plasma-liquid interface, Appl. Phys. Lett., 2018,112, 1–5.